Hindawi
Journal of Nanomaterials
Volume 2022, Article ID 6979280, 14 pages
https://doi.org/10.1155/2022/6979280

Research Article

Quantum Beat of Excitons in the Prolate Ellipsoidal Quantum Dots

Le Thi Ngoc Bao,[1] **Duong Dinh Phuoc**,[2] **Le Thi Dieu Hien**,[1,2] **and Dinh Nhu Thao**[2]

[1]*Hue University of Sciences, Hue University, 77 Nguyen Hue Street, Hue City, Vietnam*
[2]*Hue University of Education, Hue University, 34 Le Loi Street, Hue City, Vietnam*

Correspondence should be addressed to Le Thi Ngoc Bao; ltnbao@hueuni.edu.vn and Dinh Nhu Thao; dnthao@hueuni.edu.vn

Received 24 March 2022; Accepted 26 April 2022; Published 1 August 2022

Academic Editor: Nguyen Duc Cuong

In this paper, renormalized wavefunction method was applied to study quantum beats of excitons in the InGaAs/InAlAs prolate ellipsoidal quantum dots (QDs). The obtained results show that, without the pump laser, the exciton absorption intensity is just a smooth curve. In contrast, when the system is illuminated by a strong pump laser resonating with two exciton levels, the oscillation behavior of exciton absorption intensity, which is known as quantum beats of excitons, is observed. That result can be interpreted as an indirect consequence of the Pauli exclusion principle leading to a splitting of the electron levels, which forms two close exciton levels, and if two excitons are excited coherently, the interference of these two excitons will finally form a quantum beat. The study also shows that the geometry shape of the QDs has strong influence on the properties of quantum beats. Changing the period of quantum beats in particular or optical properties in general in QDs thus becomes more flexible through changing their geometry shapes. This is one interested advantage of the ellipsoidal QDs and is expected to increase their applicability more than the spherical QDs.

1. Introduction

Presently, low-dimensional semiconductors attract the attention of several researchers, thanks to their high applicability. In low-dimensional semiconductor systems, particles are confined in one dimension-quantum wells, two dimensions-quantum wires, and three dimensions-quantum dots (QDs). It is this quantum confinement that makes low-dimensional semiconductor systems, especially QDs, offer many effects with considerable potential in the manufacture of new optical devices [1]; in electronic and optoelectronic applications [2, 3]; for quantum-functional and memory devices [4, 5]; and many other research fields such as quantum computing, photovoltaics, infrared photodetectors, medical imaging, and biosensors [6–12].

Recent studies on coupled optical properties in QDs with simple shapes, such as cubic, cylindrical, and spherical QDs have been carried out [13–16]. These works show that optical properties of QDs depend to a great extent on external fields and the size of QDs. Especially, the shape of QDs also makes a notable difference to their optical properties [17, 18]. This suggests that specially shaped QDs like ellipsoidal ones can possess interestingly different optical properties. In ellipsoidal QDs, the quantized energy levels of particles are highly dependent on structural parameters [19–23]. Therefore, the optical properties in these quantum dot structures are said to be easily modifiable by these structural parameters.

Thanks to its high applicability, especially in manufacture of quantum computer, quantum beat in low-dimensional structures has attracted much attention. Using ultrashort laser pulses with various experiments [24–30], scientists have observed quantum beats of excitons in different semiconductor structures. Theoretically, scientists have applied many methods to study the quantum beats of excitons in quantum structures [25, 31–36], of which the most convenient is the renormalized wavefunction method [32, 35, 36].

In this paper, we used the renormalized wavefunction method to study the existence of quantum beats of excitons in $In_{0.53}Ga_{0.47}As/In_{0.52}Al_{0.48}As$ prolate ellipsoidal

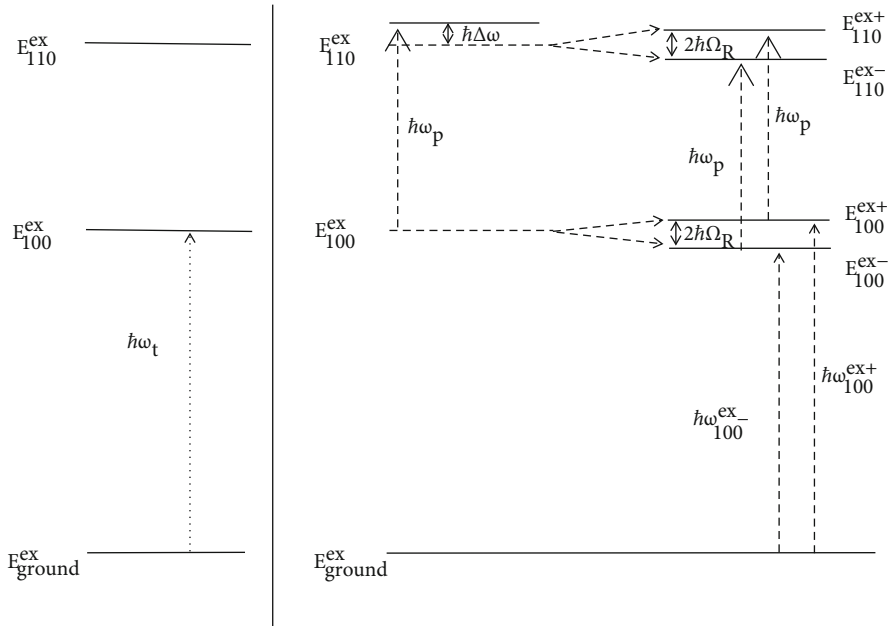

Figure 1: A three-level energy diagram and exciton transitions: (a) without the pump laser, the system contains three levels of exciton: the ground level E^{ex}_{ground} and two excited ones E^{ex}_{100}, E^{ex}_{110}. The probe laser $\hbar\omega_t$ only identifies the transition for the pair of levels $(E^{ex}_{\text{ground}}, E^{ex}_{100})$ (marked by a dotted arrow); (b) under the effect of the resonant strong pump laser coupling to the initial excited levels of exciton, E^{ex}_{100} is split into E^{ex-}_{100} and E^{ex+}_{100}; E^{ex}_{110} is separated to E^{ex-}_{110} and E^{ex+}_{110}. The probe laser $\hbar\omega_t$ identifies two transitions for two pairs of levels $(E^{ex}_{\text{ground}}, E^{ex-}_{100})$ and $(E^{ex}_{\text{ground}}, E^{ex+}_{100})$, obeying the selection rules for interband transitions (marked by thin dashed arrows).

quantum dots. We chose these heterostructures because they have the large conduction-band discontinuity between $In_{0.53}Ga_{0.47}As/In_{0.52}Al_{0.48}As$ layers that is $\Delta E_c = 500$ meV [37]. This can be approximated as the infinite confinement potential for electrons in these quantum structures, which is consistent with our hypothesis. Besides, these heterostructures have many applications [37], as well as create modern infrared devices [38, 39]. This article focuses on investigating the dependence of the exciton absorption intensity on the external fields, sizes, and shapes of quantum dot. The article includes the following main sections: Section 2 is about the model and theory, Section 3 provides the main results and discussion, and Section 4 presents the conclusions.

2. Model and Theory

2.1. Wavefunctions and Energy Levels of Exciton

2.1.1. The Case without the Pump Laser. In this case, we investigate quantum beats of excitons in prolate ellipsoidal QDs. We use a three-level diagram of exciton, including one ground level E^{ex}_{ground} and two excited ones of exciton E^{ex}_{100} and E^{ex}_{110} (Figure 1). These exciton levels are originated from interband transitions between the lowest level of hole E^{h}_{100} and the two lowest ones of electron E^{e}_{100} and E^{e}_{110} in QDs (see Figure 10(a) in Appendix A). For simplicity, we assume the prolate ellipsoidal QDs lied in an infinite potential (see Appendix A).

First, we find the stationary wavefunctions of the exciton and the corresponding energy levels in the absence of the pump laser. The wavefunctions of the exciton in the stationary states, in a strong confinement regime, are the combination of the one-particle total wavefunctions of the electron and the hole (see Equation (A.15)).

$$\begin{cases} \Lambda^{ex}_{100}\left(\vec{r}\right) = \Lambda^{e}_{100}\left(\vec{r}\right).\Lambda^{h}_{100}\left(\vec{r}\right), \\ \Lambda^{ex}_{110}\left(\vec{r}\right) = \Lambda^{e}_{110}\left(\vec{r}\right).\Lambda^{h}_{100}\left(\vec{r}\right). \end{cases} \tag{1}$$

The corresponding exciton energy levels are determined by the sum of the quantized levels of electrons E^{e}_{nlm} and holes E^{h}_{nlm} (see Equation (A.16) and Equation (A.17) in Appendix A), minus the exciton binding energy E_{binding}

$$\begin{cases} E^{ex}_{100} = E^{e}_{100} + E^{h}_{100} - E_{\text{binding}}, \\ E^{ex}_{110} = E^{e}_{110} + E^{h}_{100} - E_{\text{binding}}, \end{cases} \tag{2}$$

where E_{binding} is usually considerable smaller than the energy levels of electrons and holes. To investigate the characteristics of quantum beats with time, we utilize the time-dependent stationary wavefunctions given in the form

$$\begin{cases} \Lambda^{ex}_{100}\left(\vec{r}, t\right) = \Lambda^{ex}_{100}\left(\vec{r}\right)e^{-i/\hbar E^{ex}_{100}t}, \\ \Lambda^{ex}_{110}\left(\vec{r}, t\right) = \Lambda^{ex}_{110}\left(\vec{r}\right)e^{-i/\hbar E^{ex}_{110}t}. \end{cases} \tag{3}$$

2.1.2. The Case with the Pump Laser. In this case, we examine a system subjected to a pump laser resonating with

two exciton excited levels in the initial stationary states E^{ex}_{100} and E^{ex}_{110}. Under the effect of the pump laser, the excitons are now no longer in the initial stationary states but in the nonstationary state which is described by the product of the wavefunctions of the electron in the mixed state $\Lambda^{e}_{\text{mix}}(\vec{r},t)$ (Equation (A.26)) and the initial wavefunction of hole $\Lambda^{h}_{100}(\vec{r},t)$ (see Equation (A.18))

$$\Lambda^{ex}_{\text{mix}}\left(\vec{r},t\right)=\Lambda^{e}_{\text{mix}}\left(\vec{r},t\right).\Lambda^{h}_{100}\left(\vec{r},t\right), \tag{4}$$

The wavefunction in Equation (4) can be written in the explicit form

$$\begin{aligned}\Lambda^{ex}_{\text{mix}}\left(\vec{r},t\right)=&\frac{1}{2\Omega_R}\left(\alpha_1 e^{i\alpha_2 t}+\alpha_2 e^{-i\alpha_1 t}\right)e^{-i/\hbar E^{ex}_{100}t}\Lambda^{ex}_{100}\left(\vec{r}\right)\\&-\frac{V_{21}}{2\Omega_R\hbar}\left(e^{i\alpha_1 t}-e^{-i\alpha_2 t}\right)e^{-i/\hbar E^{ex}_{110}t}\Lambda^{ex}_{110}\left(\vec{r}\right),\end{aligned} \tag{5}$$

or it can be rewritten as

$$\begin{aligned}\Lambda^{ex}_{\text{mix}}\left(\vec{r},t\right)=&\frac{1}{2\Omega_R}\left(\alpha_1 e^{-i/\hbar E^{ex-}_{100}t}+\alpha_2 e^{-i/\hbar E^{ex+}_{100}t}\right)\Lambda^{ex}_{100}\left(\vec{r}\right)\\&-\frac{V_{21}}{2\hbar\Omega_R}\left(e^{-i/\hbar E^{ex-}_{110}t}-e^{-i/\hbar E^{ex+}_{110}t}\right)\Lambda^{ex}_{110}\left(\vec{r}\right),\end{aligned} \tag{6}$$

in which

$$\begin{cases}E^{ex+}_{100}=E^{ex}_{100}+\hbar\alpha_1,\\E^{ex-}_{100}=E^{ex}_{100}-\hbar\alpha_2,\end{cases} \tag{7}$$

and

$$\begin{cases}E^{ex+}_{110}=E^{ex}_{110}+\hbar\alpha_2,\\E^{ex-}_{110}=E^{ex}_{110}-\hbar\alpha_1,\end{cases} \tag{8}$$

and $\Lambda^{ex}_{100}(\vec{r})$ and $\Lambda^{ex}_{110}(\vec{r})$ are the stationary exciton wavefunctions when the pump laser does not turn on (Equation (1)). Equation (8) can be written as

$$\begin{cases}E^{ex+}_{110}=E^{ex+}_{100}+\hbar\omega_p,\\E^{ex-}_{110}=E^{ex-}_{100}+\hbar\omega_p.\end{cases} \tag{9}$$

From Equations (7) and (8), we have

$$\begin{cases}E^{ex+}_{100}-E^{ex-}_{100}=2\hbar\Omega_R,\\E^{ex+}_{110}-E^{ex-}_{110}=2\hbar\Omega_R.\end{cases} \tag{10}$$

Under the effect of the pump laser, the two initial excited levels of exciton split into four new energy levels in which two levels E^{ex-}_{100} and E^{ex+}_{100} are separated from level E^{ex}_{100}, and two levels E^{ex-}_{110} and E^{ex+}_{110} are separated from level E^{ex}_{110} (see Figure 1(b)). We see that the energy difference between two splitting levels E^{ex-}_{100} and E^{ex+}_{100} or between two splitting ones E^{ex-}_{110} and E^{ex+}_{110} is equal to $2\hbar\Omega_R$ (Equation (10)), which is much smaller than the photon energy of the pump laser $\hbar\omega_p$. This photon energy is also the energy distance between two pairs of levels $(E^{ex-}_{100},E^{ex+}_{100})$ and $(E^{ex-}_{110},E^{ex+}_{110})$ (Equation (9)). The Rabi frequency Ω_R is proportional to the detuning of the pump laser as well as the transition matrix element for the intersubband transition and has the following form

$$\Omega_R=\sqrt{\left(\frac{\Delta\omega}{2}\right)^2+\frac{|V_{21}|^2}{\hbar^2}}, \tag{11}$$

where $\hbar\Delta\omega$ is the detuning of the pump laser with two levels of electron E^{e}_{100} and E^{e}_{110}, and V_{21} is the matrix element for the intersubband transition between electron levels (see Equation (A.25) in Appendix A).

2.2. Absorption Intensity of Excitons

2.2.1. The Case without the Pump Laser. The existence of the quantum beats of excitons is determined through the oscillatory behavior of the absorption intensity of excitons. On the other hand, the absorption intensity is a function of the transition matrix element among the levels of exciton. Therefore, we need to compute the dipole transition matrix element among the states of exciton, first among levels of exciton in the stationary states (Figure 1(a)). Since there are two excited states of exciton in the system, when the system is illuminated by a probe laser, we would expect to obtain two transitions of exciton from the ground state $|0\rangle$ corresponding to level E^{ex}_{ground} to two initial excited states of exciton corresponding to two exciton levels E^{ex}_{100} and E^{ex}_{110}. However, according to the selection rule for the interband transition in QDs, only the exciton transition from the ground level E^{ex}_{ground} to the lowest excited level of exciton E^{ex}_{100} exists as described by the dotted arrow in Figure 1(a). Thus, in the absence of the effect of the pump laser, the permitted transition matrix element between levels E^{ex}_{ground} and E^{ex}_{100} under the action of a probe laser has the form

$$\begin{aligned}T^{ex}_{100}&=\left\langle\Lambda^{ex}_{100}\left(\vec{r},t\right)\left|\widehat{H}_{\text{int}}\right|0\right\rangle\\&=-\frac{eA_t e^{-i\omega_t t}}{m_0 i\omega_t}\left\langle\Lambda^{ex}_{100}\left(\vec{r},t\right)\left|\vec{n}.\widehat{\vec{p}}\right|0\right\rangle,\end{aligned} \tag{12}$$

where A_t and ω_t are, respectively, the amplitude and the frequency of the probe laser. Replace Equations (3) and (1) into Equation (12); we have

$$T^{ex}_{100}=-\frac{eA_t p_{cv}}{m_0 i\omega_t}e^{i/\hbar\left(E^{e}_{100}+E^{h}_{100}-\hbar\omega_t\right)t}\left\langle\Psi^{e}_{100}\left(\vec{r}\right)\Psi^{h}_{100}\left(\vec{r}\right)|0\right\rangle,, \tag{13}$$

where p_{cv} is the polarization matrix element between conduction and valence bands

$$p_{cv}=\left\langle u_c\left|\vec{n}.\widehat{\vec{p}}\right|u_v\right\rangle. \tag{14}$$

From that, we find the expression for the exciton absorption intensity when the pump laser does not turn on as

$$I_{100}^{ex}(t) \propto |T_{100}^{ex}|^2 = \left(\frac{eA_t p_{cv}}{m_0 \omega_t}\right)^2. \tag{15}$$

Because the exciton lifetime on the excited levels is finite, the excited states of exciton will fade over time. To account for the decay of $I_{100}^{ex}(t)$, we phenomenologically provide a decay parameter $\gamma = 1/T_1$ in Equation (15). From that, we obtain the expression of the absorption intensity of excitons in the absence of the pump laser as follows

$$I_{100}^{ex}(t) \propto \left(\frac{eA_t p_{cv}}{m_0 \omega_t}\right)^2 \exp(-\gamma t), \tag{16}$$

where T_1 is the lifetime of exciton on the energy level E_{100}^{ex}.

2.2.2. The Case with the Pump Laser. From Section 2.1.2, we see that exciton will stay in the nonstationary state $\Lambda_{\text{mix}}^{ex}(\vec{r}, t)$ when QDs are irradiated by a strong pump laser resonant with two initial exciton levels E_{100}^{ex} and E_{110}^{ex}. Now, to find the absorption intensity of excitons, we need to calculate the dipole transition matrix element between the ground state $|0\rangle$ and the nonstationary exciton one $\Lambda_{\text{mix}}^{ex}(\vec{r}, t)$. The matrix element in this case has the form

$$\begin{aligned} T_{\text{mix}}^{ex} &= \left\langle \Lambda_{\text{mix}}^{ex}\left(\vec{r}, t\right) \middle| \hat{\text{H}}_{\text{int}} \middle| 0 \right\rangle \\ &= -\frac{eA_t e^{-i\omega_t t}}{m_0 i \omega_t} \left\langle \Lambda_{\text{mix}}^{ex}\left(\vec{r}, t\right) \middle| \vec{n}.\widehat{\vec{p}} \middle| 0 \right\rangle. \end{aligned} \tag{17}$$

Combining Equations (6) and (17), we get the following matrix element

$$\begin{aligned} T_{\text{mix}}^{ex} = -\frac{eA_t e^{-i\omega_t t}}{m_0 i \omega_t} &\left[\frac{1}{2\Omega_R} \left(\alpha_1 e^{-i/\hbar E_{100}^{ex-} t} + \alpha_2 e^{-i/\hbar E_{100}^{ex+} t}\right)^* \right. \\ &\times \left\langle \Lambda_{100}^{ex}\left(\vec{r}\right) \middle| \vec{n}.\widehat{\vec{p}} \middle| 0 \right\rangle - \frac{V_{21}^*}{2\Omega_R \hbar} \left(e^{-i/\hbar E_{110}^{ex-} t} - e^{-i/\hbar E_{110}^{ex+} t}\right)^* \\ &\left. \times \left\langle \Lambda_{110}^{ex}\left(\vec{r}\right) \middle| \vec{n}.\widehat{\vec{p}} \middle| 0 \right\rangle \right]. \end{aligned} \tag{18}$$

Because of the selection rule for the interband transition in QDs, there are only the dipole transitions from the ground state to the pair of the lowest splitting levels of exciton $(E_{100}^{ex-}, E_{100}^{ex+})$ that are split from the initial exciton level E_{100}^{ex}. So, we have

$$\begin{aligned} T_{\text{mix}}^{ex} = -\frac{eA_t e^{-i\omega_t t}}{m_0 i \omega_t} &\left[\frac{1}{2\Omega_R} \left(\alpha_1 e^{-i/\hbar E_{100}^{ex-} t} + \alpha_2 e^{-i/\hbar E_{100}^{ex+} t}\right)^* \right. \\ &\left. \times \left\langle \Lambda_{100}^{ex}\left(\vec{r}\right) \middle| \vec{n}.\widehat{\vec{p}} \middle| 0 \right\rangle \right], \end{aligned} \tag{19}$$

or

$$\begin{aligned} T_{\text{mix}}^{ex} = -\frac{eA_t e^{-i\omega_t t}}{m_0 i \omega_t} &\left[\frac{1}{2\Omega_R} \left(\alpha_1 e^{-i/\hbar E_{100}^{ex-} t} + \alpha_2 e^{-i/\hbar E_{100}^{ex+} t}\right)^* \right] \\ &\times \left\langle \Lambda_{100}^{e}\left(\vec{r}\right) \Lambda_{100}^{h}\left(\vec{r}\right) \middle| \vec{n}.\widehat{\vec{p}} \middle| 0 \right\rangle. \end{aligned} \tag{20}$$

Equation (20) clearly shows that, after the effect of a strong pump laser resonating with two exciton excited levels in stationary state E_{100}^{ex} and E_{110}^{ex}, then in the system, there are two optical transitions from the ground state E_{ground}^{ex} to two lowest splitting level of exciton E_{100}^{ex-} and E_{100}^{ex+} (illustrated by two thin dashed arrows in Figure 1(b)). Combining Equation (A.15) into Equation (20), we get the matrix element for the dipole transition between the ground level $|0\rangle$ and the nonstationary exciton one $\Lambda_{\text{mix}}^{ex}(\vec{r}, t)$ as follows:

$$\begin{aligned} T_{\text{mix}}^{ex} = -\frac{eA_t e^{-i\omega_t t} p_{cv}}{m_0 i \omega_t} &\left[\frac{1}{2\Omega_R} \left(\alpha_1 e^{-i/\hbar E_{100}^{ex-} t} + \alpha_2 e^{-i/\hbar E_{100}^{ex+} t}\right)^* \right] \\ &\times \left\langle \Psi_{100}^{e}\left(\vec{r}\right) \Psi_{100}^{h}\left(\vec{r}\right) \middle| 0 \right\rangle, \end{aligned} \tag{21}$$

or

$$T_{\text{mix}}^{ex} = -\frac{eA_t e^{-i\omega_t t} p_{cv}}{m_0 i \omega_t} \left[\frac{1}{2\Omega_R} \left(\alpha_1 e^{-i/\hbar E_{100}^{ex-} t} + \alpha_2 e^{-i/\hbar E_{100}^{ex+} t}\right)^* \right]. \tag{22}$$

Next, we investigate the time-resolved intensity of absorption under the effect of the resonant pump laser $I_{\text{mix}}^{ex}(t)$. From Equation (10), we see that the probe laser needs a spectral width larger than $2\hbar\Omega_R$, which is energy separation between two levels E_{100}^{ex-} and E_{100}^{ex+}, in order to excite coherently two excitons in the pair $(E_{100}^{ex-}, E_{100}^{ex+})$. In order to fully observe at least a quantum beat oscillation, the period of the quantum beat needs to be less than or equal to coherence time T_2, the time it takes for two excitons in the pair $(E_{100}^{ex-}, E_{100}^{ex+})$ to oscillate in phase. Of course, the coherence time T_2 is always less than or equal to the lifetime T_1 of exciton in the state $\Lambda_{100}^{ex}(\vec{r}, t)$ (Equation (3)). Therefore, at any given time $t < T_2$, the absorption intensity of excitons under the effect of the pump laser has the following form.

$$\begin{aligned} I_{\text{mix}}^{ex}(t) &\propto |T_{\text{mix}}^{ex}|^2 \\ &= \left(\frac{eA_t p_{cv}}{m_0 \omega_t}\right)^2 \left| \frac{1}{2\Omega_R} \left(\alpha_1 e^{-i/\hbar E_{100}^{ex-} t} + \alpha_2 e^{-i/\hbar E_{100}^{ex+} t}\right)^* \right|^2, \end{aligned} \tag{23}$$

or

$$\begin{aligned} I_{\text{mix}}^{ex}(t) \propto \left(\frac{eA_t p_{cv}}{m_0 \omega_t}\right)^2 &\left[\left(\frac{\alpha_1}{2\Omega_R}\right)^2 + \left(\frac{\alpha_2}{2\Omega_R}\right)^2 \right. \\ &\left. + 2\frac{\alpha_1}{2\Omega_R}\frac{\alpha_2}{2\Omega_R} \cos\left(\frac{E_{100}^{ex+} - E_{100}^{ex-}}{\hbar}\right) t \right]. \end{aligned} \tag{24}$$

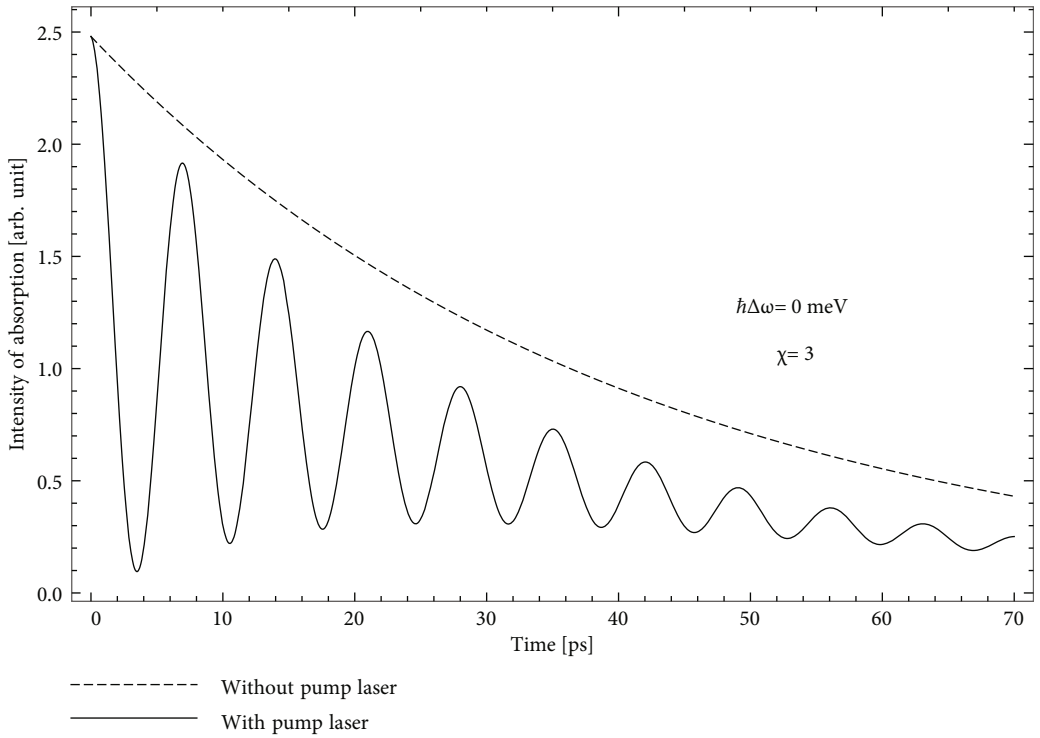

FIGURE 2: The time-dependent absorption intensity in prolate ellipsoidal QDs of the ellipsoid aspect ratio $\chi = 3$ (in consistent with the length of the semi-major axis $c = 75$ Å, satisfying the condition $2c < a_B^{ex}$) in two cases: in the absence (dashed line) and in the presence of the pump laser (solid lines) with the detuning $\hbar\Delta\omega = 0$ meV.

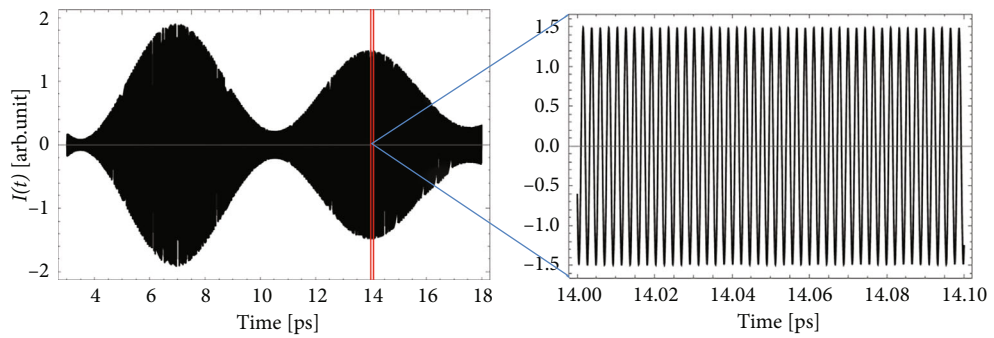

FIGURE 3: (a) The dependence of the total absorption intensity on time in the case of the ellipsoid aspect ratio $\chi = 3$. (b) An enlarged version of the curve limited by red lines.

We put

$$\begin{cases} \beta_1 = \dfrac{\alpha_1}{2\Omega_R}, \\ \beta_2 = \dfrac{\alpha_2}{2\Omega_R}, \end{cases} \tag{25}$$

and combined with Equation (10), we can rewrite the expression for the absorption intensity of excitons as

$$I_{\text{mix}}^{ex}(t) \propto \left(\frac{eA_t p_{cv}}{m_0 \omega_t}\right)^2 \left[\beta_1^2 + \beta_2^2 + 2\beta_1\beta_2 \cos\left(2\Omega_R t\right)\right]. \tag{26}$$

As mentioned in Section 2.2.1, in fact, the exciton lifetime on the excited states is finite, so the oscillation in Equation (6) decays with time. To account for damping in $I_{mix}^{ex}(t)$, we add phenomenologically the damped factors $\gamma = 1/T_1$ and $\tau = 1/T_2$ in Equation (26). From this, we obtain the final expression of the absorption intensity of excitons in the presence of the resonant pump laser as follows

$$I_{\text{mix}}^{ex}(t) \propto \left(\frac{eA_t p_{cv}}{m_0 \omega_t}\right)^2 \left[\left(\beta_1^2 + \beta_2^2\right) \exp\left(-\gamma t\right) + 2\beta_1\beta_2 \exp\left(-\tau t\right) \cos\left(2\Omega_R t\right)\right], \tag{27}$$

where T_2 is the coherent time of the state described in Equation (6).

Equation (27) shows that in the case QDs are illuminated by a probe laser in the presence of a resonant strong pump laser, the absorption intensity has the form of a

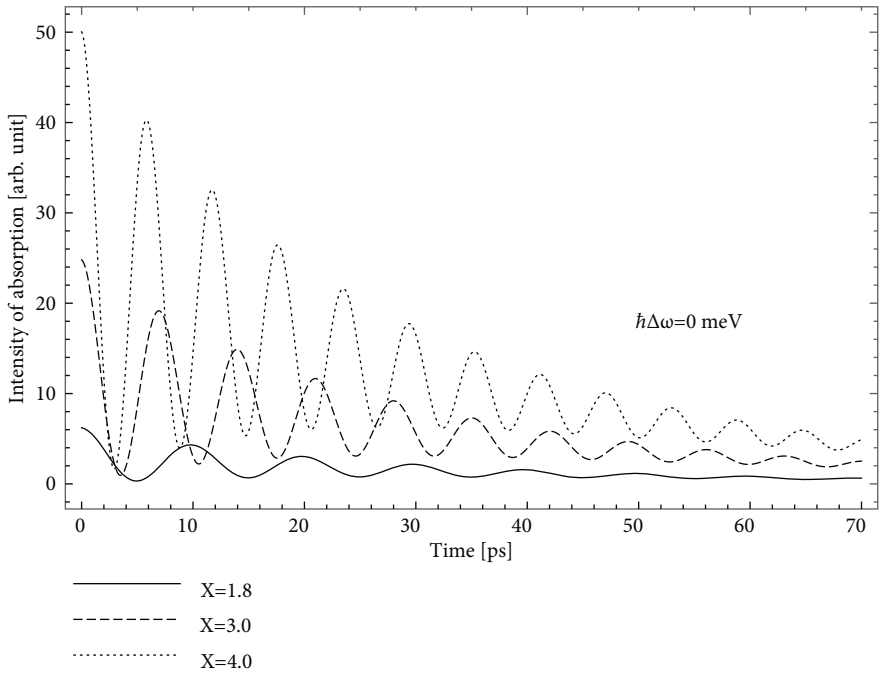

FIGURE 4: The time dependence of the absorption intensity in the prolate ellipsoidal quantum dot with different values χ: $\chi = 1.8$ (corresponding to $c = 45$ Å) is denoted by solid line, $\chi = 3$ (corresponding to $c = 75$ Å) is denoted by dashed line, and $\chi = 4$ (corresponding to $c = 100$ Å) is denoted by dotted line in the case of the effect of the pump laser with the detuning $\hbar\Delta\omega = 0$ meV.

damped periodic oscillation that owns a frequency of twice the Rabi frequency of the electron $2\Omega_R$. This oscillation indicates the existence of the quantum beats of excitons in the quantum dot structure, which we will examine and explain in detail in the next section.

As we know, when there are two oscillations of similar frequencies in the system, they will interfere with each other to form a superposition wave of the frequency that is the average of two initial frequencies (i.e., exciton ones ω_{ex}^{+} and ω_{ex}^{-}) and its amplitude oscillates with the frequency equal to one half of the difference of two initial frequencies. Thence, the beat frequency is equal to the difference of two initial frequencies. Hence, from Equation (24) or Equation (27), we can formally deduce the expression of the total absorption intensity that oscillates with the effective frequency that equal to the sum of the two initial frequencies and have the following form

$$I(t) \propto \left(\frac{eA_t p_{cv}}{m_0 \omega_t}\right)^2 \left[\left(\beta_1^2 + \beta_2^2\right) \exp\left(-\gamma t\right) + 2\beta_1\beta_2 \exp\left(-\tau t\right) \cos\left(\frac{E_{100}^{ex+} - E_{100}^{ex-}}{\hbar}\right) t\right] \cdot \cos\left(\frac{E_{100}^{ex+} + E_{100}^{ex-}}{\hbar}\right) t. \quad (28)$$

We can rewrite Equation (28) as follows

$$I(t) \propto I_{\text{mix}}^{ex}(t) \cdot \cos\left(\frac{E_{100}^{ex+} + E_{100}^{ex-}}{\hbar}\right) t. \quad (29)$$

3. Results and Discussion

To further study and demonstrate the obtained results, in this part, we perform numerical calculations for the time-resolved intensity of absorption in $In_{0.53}Ga_{0.47}As/In_{0.52}Al_{0.48}As$ prolate ellipsoidal QDs. We utilize those parameters for the calculation: the effective mass of the electron and the hole in the dot material $In_{0.53}Ga_{0.47}As$ is $m_e = 0.042m_0$ and $m_h = 0.052m_0$; the bandgap of the dot material is $E_g = 750$ meV [37, 40]; the linewidth and the amplitude of pump laser are $\Gamma = 0.1$ meV and $A_p = 4 \times 10^4$ V/cm, respectively; the lifetime of excitons is chosen as $T_1 = 40$ ps; and the coherent time T_2 is assumed to be less than the lifetime T_1 as discussed above and is chosen as $T_2 = 20$ ps.

In order to clearly study the properties of the quantum beat before the decoherence of excitons happens, laser pulses must have the pulse duration less than the decoherence time of excitons. In addition, the paper studies the prolate ellipsoidal QDs, which is a quantum structure so the major axis $2c$ and the minor axis $2a$ must have the length smaller than the bulk exciton Bohr radius in the dot material $In_{0.53}Ga_{0.47}As$, which has a value $a_B^{ex} \simeq 308$ Å. Therefore, in order to calculate, we have chosen the length of the semi-minor axis to be $a = 25$ Å; and the length of the semi-major axis will vary depending on the ellipsoid aspect ratio χ ($c = \chi \cdot a$).

First, we plot the dependence of the absorption intensity on time when the value of the ellipsoid aspect ratio of QDs is $\chi = 3$ in two cases without and with the effect of the pump laser (Figure 2). From the figure, we realize that, without the pump laser, the absorption intensity of excitons is just

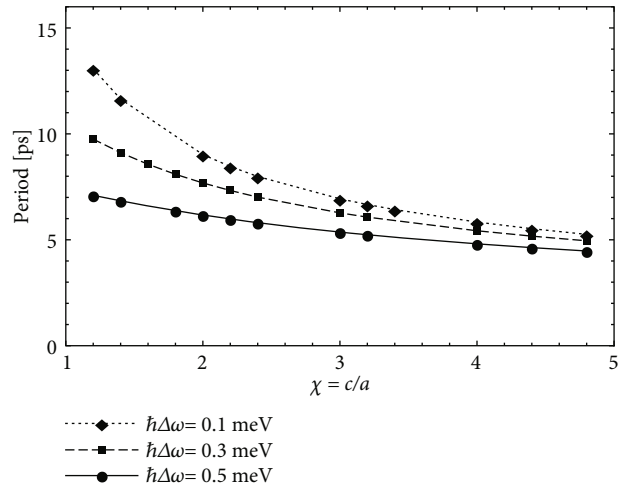

Figure 5: The period of quantum beat versus the ellipsoid aspect ratio χ with various detuning values: $\hbar\Delta\omega = 0.1$ meV (dotted line), $\hbar\Delta\omega = 0.3$ meV (dashed line), and $\hbar\Delta\omega = 0.5$ meV (solid line).

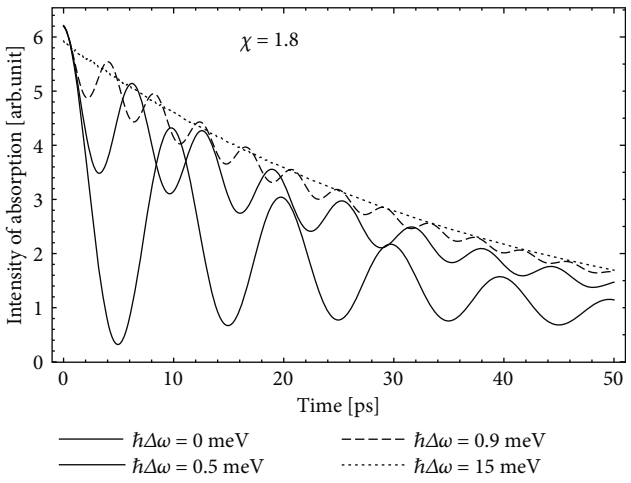

Figure 6: The time dependence of the absorption intensity in the prolate ellipsoidal quantum dot in the case of the ellipsoid aspect ratio χ =1.8 with various detuning values: $\hbar\Delta\omega = 0$ meV (thick solid line), $\hbar\Delta\omega = 0.5$ meV (thin solid line), $\hbar\Delta\omega = 0.9$ meV (dashed line), and $\hbar\Delta\omega = 15$ meV (dotted line).

a smooth curve gradually going to zero in time (dashed line), that is, there is no quantum beat of excitons. However, if we irradiate a resonant strong pump laser to connect two initial exciton levels ($\hbar\Delta\omega = 0$meV), we find the absorption intensity oscillating with the constant frequency, which is equal to twice the electron Rabi frequency $2\Omega_R$, and fading over time (the solid line). This is the quantum beat of excitons in prolate ellipsoidal QDs, like the similar to quantum beat of excitons obtained in the previously studied spherical quantum dot, quantum well, and quantum wire structures [35, 36, 41]. We find that the results obtained in prolate ellipsoidal QDs are similar to ones of spherical QDs [35], it is explained as both spherical and prolate ellipsoidal QDs belong to quasi-zero-dimensional systems.

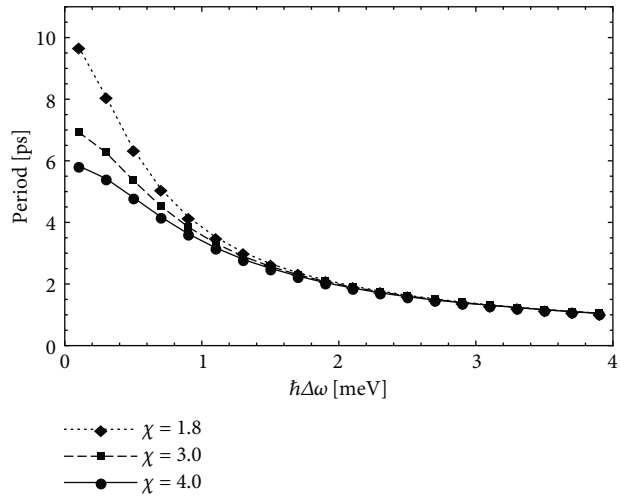

Figure 7: The period of quantum beat versus the laser detuning for various χ values: $\chi = 1.8$ (dotted line), $\chi = 3$ (dashed line), and $\chi = 4$ (solid line).

The existence of the quantum beat can be interpreted as follows. Initially, when the system is not irradiated by the pump laser, in the system, there existed two electron quantization energy levels, and according to the Pauli exclusion principle, these energy levels existed four permitted states of electron. Afterward, if the system is subjected to a strong pump laser resonant with two electron-quantized levels, those levels couple to each other and form a unique level. That new one, to obey the Pauli exclusion principle, allows only two electron states while the system needs four ones, leading to the lack of allowed electron states. To have enough number of the allowed states, each initial electron level must separate into two splitting levels as illustrated in Figure 1(b). Consequently, under the influence of the probe laser, in the absorption spectrum, we observed two interband transitions between the hole level and two splitting levels of electron (marked by thin dashed arrows in Figure 1(b)). Those transitions result in two closely spaced exciton levels, similar to the results obtained before in other quantum structures [16, 18]. Since these two exciton levels have roughly the same frequency, when they oscillate in phase, they will interfere with each other to form a quantum beat [35, 36], as showed in Figure 3 below.

Starting from Equation (28), we plot the total absorption intensity with the effective frequency that equal to the sum of the two exciton frequencies ω_{ex}^{+} and ω_{ex}^{-} as shown in Figure 3. Here, we add the absorption intensity of quantum beat to the total absorption intensity as described by Equation (29). In addition, the absorption intensity of quantum beat changes with time and oscillates with the frequency being twice the electron Rabi frequency, as described by the solid lines ὁ Figure 2.

Next, to find out the characteristics of the quantum beat of excitons, we examine the dependence of the absorption intensity of excitons on the ellipsoid aspect ratio. Figure 4 shows the dependence of the absorption intensity over time for different values of the ellipsoid aspect ratio χ. In all three cases, we observe a damped oscillation of the absorption

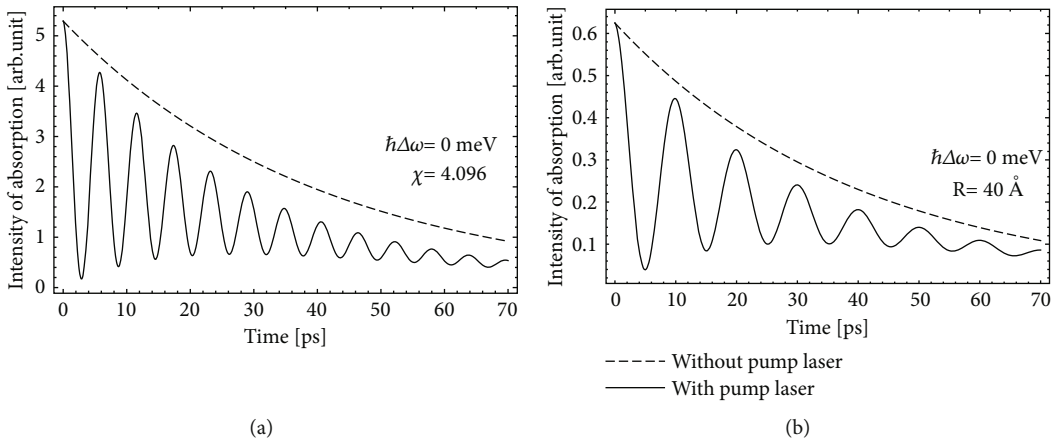

Figure 8: The dependence of the absorption intensity of excitons over time: (a) in the prolate ellipsoidal QD with the length of the semi-minor axis $a = 25$ Å, $\chi = 4.096$ (in consistent with the length of the semi-major axis $c = 102.4$ Å) and (b) in the spherical QD with radius $R = 40$ Å of the same volume.

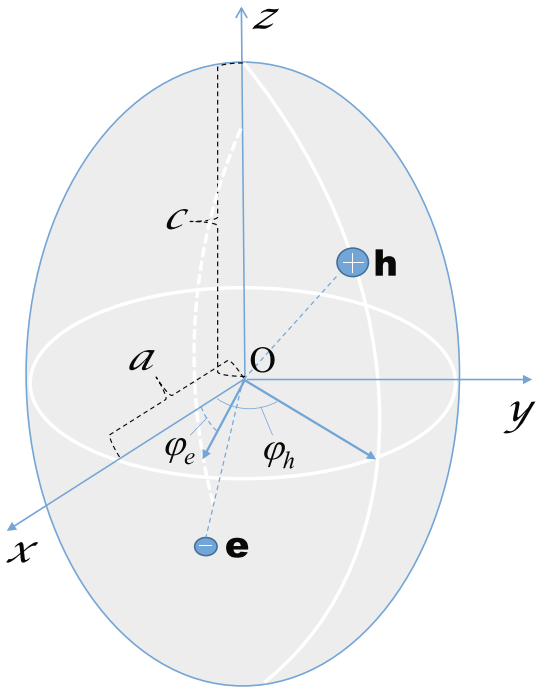

Figure 9: Electron-hole pair in a prolate ellipsoidal QD.

intensity, confirming the existence of the quantum beat of excitons. Besides, investigation shows that the oscillation of the absorption intensity strongly depends on the ellipsoid aspect ratio χ. As the value of the ellipsoid aspect ratio χ increases, so does the amplitude and frequency of the oscillation. This means that as the value χ increases, the stronger quantum beat phenomenon appears, and the greater oscillation frequency is. This can be explained as follows.

According to Equation (A.16) and Equations (A.6), (A.8), and (A.11), electron quantization energy levels E^e_{100} and E^e_{110} are inversely proportional to the ellipsoid aspect ratio χ. Therefore, when we increase the value of the ellipsoid aspect ratio χ, then the separation between the two electron levels becomes smaller or, in other words, the electron energy levels shift closer, that is, the transition probability between these two levels will increase (or V_{21} increases). Therefore, when a resonant pump laser is turned on, each initial electron level must immediately split into two new levels in order to comply with the Pauli exclusion principle. Then, if we irradiate a suitable probe laser into the system, we will see the transitions from the hole energy level to these new energy levels of the electron. As a result, excitons are rapidly generated, and since they are at roughly equal levels, a quantum beat of excitons is quickly formed. Otherwise, according to the quantum size effects, we have ω_t being a decreasing function of χ, and from Equation (27), we again have the beat amplitude inversely proportional with frequency of the probe photon ω_t. Therefore, as the ellipsoid aspect ratio χ increases, so does the beat amplitude. In brief, the more we increase the value of χ, the closer the initial energy levels of the electron are to each other and the easier it is for the corresponding states to couple to each other. Consequently, the more likely the splitting of the electron levels is to occur, and the more rapidly the quantum beat of excitons forms, the higher the amplitude of quantum beat as a result. Besides, according to Equation (11), the electron Rabi frequency is proportional to the transition matrix element V_{21}. Also, as mentioned above, as we increase the value of χ, the transition probability between two electron quantized levels increases (or V_{21} increases). As a result, when we increase the value of χ, the electron Rabi frequency increases, so the oscillatory frequency of quantum beat also increases because the oscillatory frequency of beat is twice the electron Rabi frequency.

To study more clearly the feature of the quantum beat period, in Figure 5, we plot the quantum beat period versus the ellipsoid aspect ratio χ with different detuning values. We see that in all three cases when increasing χ, the quantum beat period decreases (or the quantum beat frequency increases as argued above) and approaches the same value which is said to be the period of quantum beat in the bulk semiconductor. In addition, we see that as the detuning increases, the quantum beat period decreases accordingly.

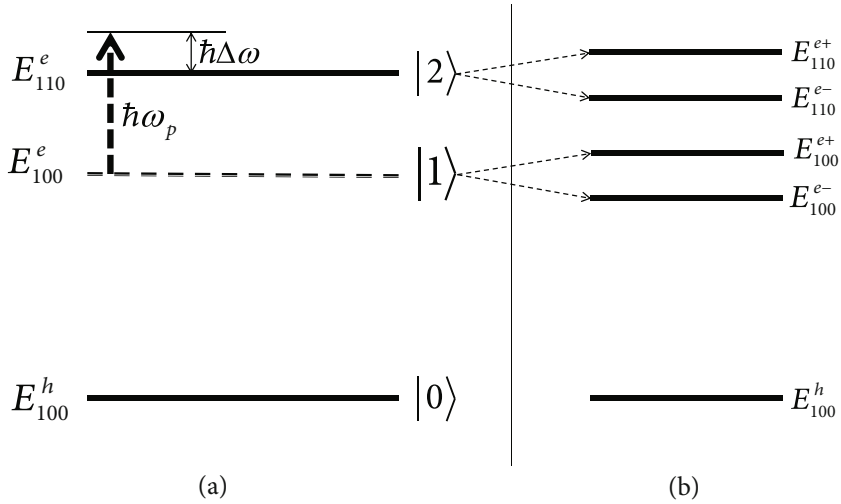

Figure 10: Three-level energy diagram of electron and hole: (a) before the effect of the pump laser. E^h_{100} is the lowest quantized energy level of the hole corresponding to the state $|0\rangle$; E^e_{100} and E^e_{110} are the first quantized levels of the electron corresponding to the states $|1\rangle$ and $|2\rangle$. (b) After the system is illuminated by a strong resonant pump laser with the photon energy $\hbar\omega_p \simeq E^e_{110} - E^e_{100}$, electron energy levels are split: E^e_{100} is split into E^{e-}_{100} and E^{e+}_{100}, E^e_{110} is split into E^{e-}_{110} and E^{e+}_{110}; $\hbar\Delta\omega$ is the detuning of the pump wave and the two quantized levels of the electron.

This relationship will be discussed in detail in the scenario of Figure 6.

Figure 6 examines the dependence of the feature of quantum beat of excitons on the pump field detuning. We see that as the detuning increases, both the period and the amplitude of quantum beat decrease. It is clear that as the detuning increases, the coupling probability of two electron energy level lowers, leading to a decrease in the splitting of the electron energy levels as well as a decrease in the ability to generate two closely spaced excitons. As a result, the probability of generating quantum beats decreases, leading to a smaller amplitude of quantum beat. Besides, according to Equation (11), the oscillation frequency of beat is proportional to the detuning so when we increase the detuning, the oscillation frequency of beat increases, or the oscillatory period of quantum beat decreases. Notably, when the detuning is too large, we cannot observe the oscillation of the absorption intensity over time, that is, the quantum beat of excitons does not appear (corresponding to $\hbar\Delta\omega = 15$ meV represented by the dotted line in Figure 7).

Next, we examine the relation between the period of quantum beat and the detuning of the pump wave (Figure 7). The graph in Figure 7 reveals that when the detuning increases, the period of quantum beat decreases as mentioned above and that periods of various detuning values approach the same value that is said to be the oscillatory period of the initial excitons. In addition, we see that the period of quantum beat decreases with the increasing value of the ellipsoid aspect ratio χ as explained in the discussion of Figure 6. Compared to spherical quantum dots, which have only radius to work with, ellipsoidal QDs have more adjustable geometrical parameters such as semi-minor axis and semi-major axis. It makes easier for one to adjust and obtain desired optical properties in more detailed exciton energy spectrum [42, 43].

Finally, we compare the absorption intensity of excitons in the prolate ellipsoidal QD Figure 8(a)) and the spherical one (Figure 8(b)) [35] with the same volume. Starting from Equation (A.14), we consider the prolate ellipsoidal QD with $a = 25$ Å and $\chi = 4.096$ that has the same volume as the spherical one with radius $R = 40$ Å. The graph in Figure 8 shows that the characteristics of the quantum beat of excitons in two QDs of different shapes but having the same volume are completely different. This means that the quantum beat of excitons depends not only on the pump laser detuning, size of QDs but also on their geometric shapes. The reason for the difference between the feature of the quantum beat in those two kinds of QDs can be explained as follows. As we know, the shape of the QDs strongly influences the wavefunctions as well as the energy spectrum of particles. So, for two QDs with different shapes, the wavefunctions and the corresponding energy spectra are completely different, even though the QDs have the same volume. This results in the photon energy of the probe laser necessary to excite interband transitions in the prolate ellipsoidal QDs being different from that in the spherical ones, that is, the absorption intensity of excitons in these QDs is different. In addition, in this paper, we use the renormalized wavefunction method based on the theory of quantum mechanics, so our formulation can be applied to other quantum structures as long as we can define the wavefunctions and energy spectrum of particles. In fact, we have applied our theory to similar problems in the spherical QDs as well as in quantum wires and quantum wells [16, 18, 35, 36, 41].

4. Conclusion

In this work, we have studied quantum beats of excitons in InGaAs/InAlAs prolate ellipsoidal QDs using a three-level model by the renormalized wavefunctions method. We have

found the form of the renormalized wavefunction of exciton and calculated the absorption intensity of excitons in two cases without and with the effect of the pump laser. In the presence of a resonant pump laser, the time-dependent spectrum of the exciton absorption intensity has the form of a damped periodic oscillation with a frequency being twice the electron Rabi frequency. That oscillatory behavior of the exciton absorption intensity reveals the existence of quantum beats in these QDs. The amplitude and frequency (or period) of quantum beats depend very sensitively on the detuning as well as the ellipsoid aspect ratio. The semi-minor axis and semi-major one have made controlling optical properties in ellipsoidal QDs easier and more flexible than in the spherical QDs. This is one interesting advantage of the ellipsoidal QDs over spherical ones. Moreover, the features of quantum beats of excitons also depend sensitively on geometric shapes of QDs. Specifically, with the same volume, the frequency and amplitude of quantum beats in the two spherical and prolate ellipsoidal QDs are completely different. We believe that the interesting features in optical absorption of QDs when the quantum beat of excitons occurs will have great potential for application in manufacturing quantum-computing devices. We expect our findings to be confirmed by further appropriate experiments.

Appendix

For the sake of convenience, we recall here the wavefunctions and the energy spectra of electron and hole in prolate ellipsoidal quantum dots (QDs) [18–22]. Consider the prolate ellipsoidal QD with rotational symmetry around the z axis. Let a and c be the length of semi-axes of the ellipse in the xOy plane and z-direction, respectively, where x, y, z are the coordinates in Cartesian coordinate system with its origin at the ellipsoid symmetry center. For simplicity, we have assumed the prolate ellipsoidal QD is in an infinite potential and has the form [18–22]

$$U\left(\vec{r}\right) = \begin{cases} 0, & 0 < S\left(\vec{r}_i\right) < 1, \\ \infty, & S\left(\vec{r}_i\right) \geq 1, \end{cases} \tag{A.1}$$

where $S(\vec{r}_i)$ depends on parameters a and c which are the semi-axes of the ellipsoidal QD; we have

$$S\left(\vec{r}_i\right) = \frac{x^2 + y^2}{a^2} + \frac{z^2}{c^2}, \tag{A.2}$$

with $c > a$, we have the prolate ellipsoidal QD as shown in Figure 9.

The envelope wavefunctions of electron (hole) in prolate ellipsoidal QD have the form [19–23]

$$\Psi_{nlm}^{e,h}(\xi, \eta, \varphi) = A_{nlm} J_{lm}^{(1)}(h, \xi) S_{lm}^{(1)}(h, \eta) e^{im\varphi}, \tag{A.3}$$

where $n = 1, 2, 3, \cdots$; $l = 0, 1, 2, 3, \cdots$; $m = -l, \cdots, 0, \cdots, +l$; $J_{lm}^{(1)}(h, \xi)$ and $S_{lm}^{(1)}(h, \xi)$ are prolate radial and prolate angular spheroidal functions of the first kind, respectively; A_{nlm} is the normalization coefficient

$$A_{nlm} = \sqrt{\frac{\chi^3}{2\pi c^3 e^3 \int_1^{\bar{\xi}} \int_{-1}^{+1} \left(\xi^2 + \eta^2\right) J_{lm}^{(1)*}(h, \xi) S_{lm}^{(1)*}(h, \eta) J_{lm}^{(1)}(h, \xi) S_{lm}^{(1)}(h, \eta) d\xi d\eta}}, \tag{A.4}$$

where

$$\chi = \frac{c}{a}, \tag{A.5}$$

and e is the ellipsoid eccentricity

$$e = \sqrt{1 - \frac{1}{\chi^2}}. \tag{A.6}$$

The energy of electron (hole) is given as

$$\varepsilon_{nlm}^{e,h} = \frac{\hbar^2 k_{nlm}}{2m_{e,h}^*}, \tag{A.7}$$

where

$$k_{nlm} = \frac{h^2}{f^2}. \tag{A.8}$$

The values of h are found from the boundary condition

$$J_{lm}^{(1)}\left(h, \bar{\xi}\right) = 0, \tag{A.9}$$

where

$$\bar{\xi} = \frac{1}{\sqrt{1 - 1/\chi^2}} = \frac{1}{e}, \tag{A.10}$$

$$f = \frac{c}{\bar{\xi}} = c \cdot e. \tag{A.11}$$

The values of the parameter h depend on the values of the indices n, l, m. When $h \longrightarrow 0$ (or $f \longrightarrow 0$, the prolate ellipsoidal QD will become the spherical one and $\chi \longrightarrow 1$. Then, the wavefunctions of electron (hole) in QD will have the following form [44]

$$\Psi_{nlm}^{S(e,h)}(r,\theta,\varphi) = \sqrt{\frac{2}{R^3}}\frac{j_l(\chi_{nl}(r/R))}{j_{l+1}(\chi_{nl})}Y_{lm}(\theta,\varphi), \quad (A.12)$$

where $Y_{lm}(\theta,\varphi)$ is the spherical harmonic function; $j_l(r)$ is the spherical Bessel function with χ_{nl} is its zeros. The energy levels of electron (hole) being consistent with wavefunctions in Equation (A.12) are determined by

$$E_{nl}^{S(e,h)} = \frac{\hbar^2\chi_{nl}^2}{2m_{e,h}R^2}. \quad (A.13)$$

In Equations. (A.12) and (A.13), indices n, l, m are principle, orbital, and azimuthal quantum numbers, respectively. Since the spherical symmetry has been lost, for the ellipsoidal QDs, the index l in the wavefunctions and energy expressions of the particle in Equations (A.3) and (A.7) no longer means the orbital quantum numbers. However, here, we still use indices n, l, m in Equations (A.3) and (A.7) to get one-to-one correspondence between the prolate ellipsoidal and spherical QD when $\chi \longrightarrow 1$. The volume of prolate ellipsoidal QD of semi-axes a and c is defined as

$$V = \frac{4}{3}\pi a^2 c = \frac{4}{3}\pi a^3\chi = \frac{4}{3}\pi R_S^3, \quad (A.14)$$

with $R_s = a\sqrt[3]{\chi}$ being the radius of a sphere with the same volume.

A. The Case without the Pump Laser

In the effective mass envelope-function approximation, the total wavefunction of electron (hole) in a prolate ellipsoidal QD with infinite potential is given as

$$\Lambda_{nlm}^{e,h}\left(\vec{r}\right) = u_{c,v}\left(\vec{r}\right)\Psi_{nlm}^{e,h}(\xi,\eta,\varphi), \quad (A.15)$$

where $\vec{r} = (\xi,\eta,\varphi)$ and $u_{c,v}(\vec{r})$ are the periodic Bloch functions in conduction and valence band. Choosing zero energy at the top of the valence band, the energy expression of electron and hole (in Equation (A.7)) is rewritten as follows, respectively

$$E_{nlm}^e = E_g + \frac{\hbar^2 k_{nlm}}{2m_e^*}, \quad (A.16)$$

$$E_{nlm}^h = \frac{\hbar^2 k_{nlm}}{2m_h^*}, \quad (A.17)$$

where E_g is the bandgap of the semiconductor.

We examine a three-level energy model where E_{100}^h is the lowest quantized energy level of the hole corresponding to the state $|0\rangle$; E_{100}^e and E_{110}^e are the first quantized levels of the electron corresponding to the states $|1\rangle$ and $|2\rangle$, see Figure 10(a).

Here, we need to use the time-dependent wavefunctions of the particles to find the time-dependent properties of the quantum beats. The time-dependent wavefunctions of the particles are now defined with

$$\begin{cases} \Lambda_{100}^h\left(\vec{r},t\right) = \Lambda_{100}^h\left(\vec{r}\right)e^{-i/\hbar E_{100}^h t}, \\ \Lambda_{100}^e\left(\vec{r},t\right) = \Lambda_{100}^e\left(\vec{r}\right)e^{-i/\hbar E_{100}^e t}, \\ \Lambda_{110}^e\left(\vec{r},t\right) = \Lambda_{110}^e\left(\vec{r}\right)e^{-i/\hbar E_{110}^e t}. \end{cases} \quad (A.18)$$

B. The Case with the Pump Laser

To search for the quantum beats in three-level model, we used two different laser beams concurrently. A strong pump laser resonant with two electron energy levels is irradiated to support the intersubband transition between these levels. A weak probe laser is utilized to search for the excitonic transitions between ground state and excited ones of exciton. The lasers can be described as follows:

$$\vec{E}(t) = \vec{n}A_x e^{-i\omega_x t}, \quad (A.19)$$

where $\vec{n}$ is the unit vector along the wave propagation direction; A_x and ω_x are the amplitude and frequency of lasers with x indicating which laser is pump or probe laser.

In case the electromagnetic field is not too strong, we can omit the higher-order term, and by applying some gauges and approximations, the expression for the Hamiltonian interaction between the electron and the electromagnetic field can be written as follows [44, 45].

$$\widehat{H}_{\text{int}} = -\frac{q}{m_0}\frac{A_x e^{-i\omega_x t}}{i\omega_x}\vec{n}\cdot\widehat{\vec{p}}, \quad (A.20)$$

where q, m_0, and $\vec{p}$ are the charge, the bare mass, and the momentum of the electron, respectively.

When there is the effect of strong pump laser resonating with the energy distance between the two quantized levels of the electron, the wavefunctions of the electron are renormalized under the effect of the pump laser and have the form

$$\Lambda_{\text{mix}}^e\left(\vec{r},t\right) = \sum_{l=0}^{1} c_l(t)\Lambda_{1l0}^e\left(\vec{r}\right)\exp\left(-\frac{i}{\hbar}E_{1l0}^e t\right), \quad (A.21)$$

where coefficients $c_l(t)$ $(l = \overline{0,1})$ are determined from the time-dependent Schrödinger equation and has the following expression [16]:

$$\begin{cases} c_0(t) = \dfrac{1}{2\Omega_R}\left(\alpha_1 e^{i\alpha_2 t} + \alpha_2 e^{-i\alpha_1 t}\right), \\ c_1(t) = -\dfrac{V_{21}}{2\Omega_R}\left(e^{i\alpha_1 t} - e^{-i\alpha_2 t}\right), \end{cases} \tag{A.22}$$

where

$$\begin{cases} \alpha_1 = \Omega_R - \dfrac{\Delta\omega}{2}, \\ \alpha_2 = \Omega_R + \dfrac{\Delta\omega}{2}, \\ \Omega_R = \left[\left(\dfrac{\Delta\omega}{2}\right)^2 + \dfrac{|V_{21}|^2}{\hbar^2}\right]^{1/2}, \end{cases} \tag{A.23}$$

$$\begin{cases} \Delta\omega = \omega_p - \omega_{21}, \\ \hbar\omega_{21} = E^e_{110} - E^e_{100}, \end{cases} \tag{A.24}$$

and V_{21} is the matrix element for an intersubband transition and has the form

$$\begin{aligned} V_{21} = {} & \frac{qA_p}{m_0 i\omega_p}\frac{m^*_e}{i\hbar}(E_2 - E_1)2\pi f^4 \times \\ & \times \int_1^{\bar{\xi}}\int_{-1}^{+1} \xi\eta\left(\xi^2 - \eta^2\right) J^{(1)*}_{10}(h,\xi) S^{(1)*}_{10} \\ & \cdot (h,\eta) J^{(1)}_{00}(h,\xi) S^{(1)}_{00}(h,\eta) d\xi d\eta, \end{aligned} \tag{A.25}$$

with q and m_e are the charge and the effective electron mass, $\hbar$ is Planck's constant, $f = c/\bar{\xi} = ce$; A_p, ω_p are the magnitude and the frequency of the pump laser, respectively.

Substituting coefficients $c_0(t)$ and $c_1(t)$ in Equation (A.22) into Equation (A.21), we obtain the formula for the renormalized wavefunction of electron under the effect of the pump laser as

$$\begin{aligned} \Lambda^e_{\text{mix}}\left(\vec{r}, t\right) = {} & \frac{1}{2\Omega_R}\left(\alpha_1 e^{i\alpha_2 t} + \alpha_2 e^{-i\alpha_1 t}\right) e^{-i/\hbar E^e_{100} t} \Lambda^e_{100}\left(\vec{r}\right) \\ & - \frac{V_{21}}{2\hbar\Omega_R}\left(e^{i\alpha_1 t} - e^{-i\alpha_2 t}\right) e^{-i/\hbar E^e_{110} t} \Lambda^e_{110}\left(\vec{r}\right). \end{aligned} \tag{A.26}$$

Put

$$\begin{cases} E^{e+}_{100} = E^e_{100} + \hbar\alpha_1, \\ E^{e-}_{100} = E^e_{100} - \hbar\alpha_2, \end{cases} \tag{A.27}$$

$$\begin{cases} E^{e+}_{110} = E^e_{110} + \hbar\alpha_2, \\ E^{e-}_{110} = E^e_{110} - \hbar\alpha_1. \end{cases} \tag{A.28}$$

From Equations (A.27) and (A.28), we can rewrite the renormalized wavefunctions of the electron under the effect of the pump laser in expression (A.26) as follows:

$$\begin{aligned} \Lambda^e_{\text{mix}}\left(\vec{r}, t\right) = {} & \frac{1}{2\Omega_R}\left(\alpha_1 e^{-i/\hbar E^{e-}_{100} t} + \alpha_2 e^{-i/\hbar E^{e+}_{100} t}\right) \Lambda^e_{100}\left(\vec{r}\right) \\ & - \frac{V_{21}}{2\hbar\Omega_R}\left(e^{-i/\hbar E^{e-}_{110} t} - e^{-i/\hbar E^{e+}_{110} t}\right) \Lambda^e_{110}\left(\vec{r}\right). \end{aligned} \tag{A.29}$$

It should also note that $\hbar\Delta\omega = \hbar\omega_p - \hbar\omega_{21}$ is the detuning between the pump laser and two initial levels of electron E^e_{100} and E^e_{110}. We find that those two initial levels are all split under the effect of a resonant strong pump laser, Figure 10(b). The quasienergy spectrum of electron now includes four splitting levels, where two levels are split from the first original level E^e_{100} defined in Equation (A.27), and two levels are split from the second original level E^e_{110} defined in Equation (A.28).

Data Availability

The material data used to support the findings of this study are included within the article.

Conflicts of Interest

The authors declare that they have no conflicts of interest.

Acknowledgments

This research is funded by the Vietnam's Ministry of Education and Training (MOET) under grant number B-2020-DHH-06. We would like to thank Dr. Tran Quang Ngoc Thuy, University of Foreign Languages, Hue University, Vietnam, for her kind assistance in manuscript preparation.

References

[1] K. Li, K. Guo, and L. Liang, "Effect of the shape of quantum dots on the refractive index changes," *Physica B*, vol. 502, pp. 146–150, 2016.

[2] J. Fang, Z. Zhou, M. Xiao, Z. Lou, Z. Wei, and G. Shen, "Recent advances in low-dimensional semiconductor nanomaterials and their applications in high-performance photodetectors," *InfoMat*, vol. 2, no. 2, pp. 291–317, 2020.

[3] J. Wu, S. Chen, A. Seeds, and H. Liu, "Quantum dot optoelectronic devices: lasers, photodetectors and solar cells," *Journal of Physics D: Applied Physics*, vol. 48, article 363001, pp. 1–28, 2015.

[4] L. Aderras, E. Feddi, A. Bah, F. Dujardin, and C. A. Duque, "On the electronic states in lens-shaped quantum dots," *Physica Status Solidi (b)*, vol. 254, no. 10, article 1700144, pp. 1–8, 2017.

[5] P. Dimitrakis, P. Normand, V. Ioannou-Sougleridis et al., "Quantum dots for memory applications," *Physica Status Solidi (A)*, vol. 210, no. 8, pp. 1490–1504, 2013.

[6] B. Talluri, E. Prasad, and T. Thomas, "Critical role of surfactants in the formation of digestively-ripened, ultra-small (r<2 nm) copper oxide quantum dots," *Superlattices and Microstructures*, vol. 116, pp. 122–130, 2018.

[7] S. Kaur, S. Sharma, A. Umar, S. Singh, S. K. Mehta, and S. K. Kansal, "Solar light driven enhanced photocatalytic

degradation of brilliant green dye based on ZnS quantum dots," *Superlattices and Microstructures*, vol. 103, pp. 365–375, 2017.

[8] A. Mehramiz, J. Mahmoodi, and S. Sobhanian, "Approximation method for a spherical bound system in the quantum plasma," *Physics of Plasmas*, vol. 17, article 082110, pp. 1–6, 2010.

[9] D. Kandi, S. Martha, and K. M. Parida, "Quantum dots as enhancer in photocatalytic hydrogen evolution: a review," *International Journal of Hydrogen Energy*, vol. 42, no. 15, pp. 9467–9481, 2017.

[10] M. F. Frasco and N. Chaniotakis, "Semiconductor quantum dots in chemical sensors and biosensors," *Sensors*, vol. 9, no. 9, pp. 7266–7286, 2009.

[11] K. D. Wegner and N. Hildebrandt, "Quantum dots: bright and versatile in vitro and in vivo fluorescence imaging biosensors," *Chemical Society Reviews*, vol. 44, no. 14, pp. 4792–4834, 2015.

[12] N. Hildebrandt, "Biofunctional quantum dots: controlled conjugation for multiplexed biosensors," *Acs Nano*, vol. 5, pp. 5286–5290, 2011.

[13] Q.-Y. Ye, R. Tsu, and E. H. Nicollian, "Resonant tunneling via microcrystalline-silicon quantum confinement," *Physical Review B*, vol. 44, pp. 1806–1811, 1991.

[14] V. A. Harutyunyan, E. M. Kazaryan, A. A. Kostanyan, and H. A. Sarkisyan, "Interband transitions in cylindrical layer quantum dot: influence of magnetic and electric fields," *Physica E*, vol. 36, no. 1, pp. 114–118, 2007.

[15] C.-H. Liu and B.-R. Xu, "Theoretical study of the optical absorption and refraction index change in a cylindrical quantum dot," *Physics Letters A*, vol. 372, no. 6, pp. 888–892, 2008.

[16] D. N. Thao, L. T. N. Bao, D. D. Phuoc, and N. H. Quang, "A theoretical study of the optical Stark effect in InGaAs/InAlAs quantum dots," *Semiconductor Science and Technology*, vol. 32, article 025014, pp. 1–8, 2017.

[17] L. Liang and W. Xie, "Influence of the shape of quantum dots on their optical absorptions," *Physica B*, vol. 462, pp. 15–17, 2015.

[18] L. T. N. Bao, D. D. Phuoc, L. T. D. Hien, and D. N. Thao, "On the optical stark effect of excitons in InGaAs prolate ellipsoidal quantum dots," *Journal of Nanomaterials*, vol. 2021, Article ID 5586622, 12 pages, 2021.

[19] G. Cantele, D. Ninno, and G. Iadonisi, "Confined states in ellipsoidal quantum dots," *Journal of Physics: Condensed Matter*, vol. 12, pp. 9019–9036, 2000.

[20] G. Cantele, D. Ninno, and G. Iadonisi, "Calculation of the infrared optical transitions in semiconductor ellipsoidal quantum dots," *Nano Letters*, vol. 1, no. 3, pp. 121–124, 2001.

[21] G. Cantele, G. Piacente, D. Ninno, and G. Iadonisi, "Optical anisotropy of ellipsoidal quantum dots," *Physical Review B*, vol. 66, article 113308, pp. 1–4, 2002.

[22] G. Iadonisi, G. Cantele, V. M. Ramaglia, and D. Ninno, "Electronic and optical properties of semiconductor nanostructures," *Physica Status Solidi (b)*, vol. 237, no. 1, pp. 320–340, 2003.

[23] V. I. Boichuk, V. B. Hol'skyi, R. Y. Kubay, and R. I. Lukin, "The electron energy spectrum in an ellipsoidal quantum dot with regard for finite band gap at the interface," *Ukrainian Journal of Physics*, vol. 53, pp. 574–578, 2008.

[24] E. Perfetto, D. Sangalli, A. Marini, and G. Stefanucci, "First-principles approach to excitons in time-resolved and angle-resolved photoemission spectra," *Physical Review B*, vol. 94, article 245303, pp. 1–15, 2016.

[25] A. Rustagi and A. F. Kemper, "Coherent excitonic quantum beats in time-resolved photoemission measurements," *Physical Review B*, vol. 99, article 125303, pp. 1–7, 2019.

[26] V. Trifonov, I. Ya, I. Gerlovin et al., "Multiple-frequency quantum beats of quantum confined exciton states," *Physical Review B*, vol. 92, article 201301, pp. 1–5, 2015.

[27] S. Ohta, O. Kojima, T. Kita, and T. Isu, "Observation of quantum beat oscillations and ultrafast relaxation of excitons confined in GaAs thin films by controlling probe laser pulses," *Journal of Applied Physics*, vol. 111, article 023505, pp. 1–4, 2012.

[28] K. Leo, J. Shah, E. O. Göbel et al., "Coherent oscillations of a wave packet in a semiconductor double-quantum-well structure," *Physical Review Letters*, vol. 66, no. 2, pp. 201–204, 1991.

[29] M. Koch, J. Feldmann, G. V. Plessen, E. O. Göbel, P. Thomas, and K. Köhler, "Quantum beats versus polarization interference: an experimental distinction," *Physical Review Letters*, vol. 69, no. 25, pp. 3631–3634, 1992.

[30] J. Erland and I. Balslev, "Theory of quantum beat and polarization interference in four-wave mixing," *Physical Review A*, vol. 48, no. 3, pp. R1765–R1768, 1993.

[31] M. S. C. Luo, S. L. Chuang, P. C. M. Planken, I. Brener, and M. C. Nuss, "Coherent double-pulse control of quantum beats in a coupled quantum well," *Physical Review B*, vol. 48, no. 15, pp. 11043–11050, 1993.

[32] A. I. Bobrysheva, M. I. Shmiglyuk, and V. G. Pavlov, "Optical exciton Stark effect and quantum beats at exciton quasienergy levels in quantum wells," *Physics of the Solid State*, vol. 39, no. 7, pp. 1147–1149, 1997.

[33] S. Schmitt-Rink, D. Bennhardt, V. Heuckeroth et al., "Polarization dependence of heavy- and light-hole quantum beats," *Physical Review B*, vol. 46, no. 16, pp. 10460–10463, 1992.

[34] K.-H. Pantke, P. Schillak, J. Erland, V. G. Lyssenko, B. S. Razbirin, and J. M. Hvam, "Nonlinear quantum beats of excitons in CdSe," *Physica Status Solidi (b)*, vol. 173, no. 1, pp. 91–98, 1992.

[35] D. N. Thao and L. T. N. Bao, "Quantum beat of excitons in spherical semiconductor quantum dots," *Superlattices and Microstructures*, vol. 146, article 106675, pp. 1–12, 2020.

[36] D. D. Phuoc, L. T. N. Bao, L. T. D. Hien, H. K. Hieu, and D. N. Thao, "A study on quantum beats of excitons in GaAs/AlGaAs circular cylindrical quantum wires," *Japanese Journal of Applied Physics*, vol. 59, article 125003, pp. 1–10, 2020.

[37] H. Asai and Y. Kawamura, "Intersubband absorption in $In_{0.53}Ga_{0.47}As/In_{0.52}Al_{0.48}As$ multiple quantum wells," *Physical Review B*, vol. 43, no. 6, pp. 4748–4759, 1991.

[38] K. F. Renk, *Basics of Laser Physics: For Students of Science and Engineering*, Springer, Berlin, 2nd ed. edition, 2017.

[39] M. A. Ladugin, I. V. Yarotskaya, T. A. Bagaev et al., "Advanced AlGaAs/GaAs heterostructures grown by MOVPE," *Crystals*, vol. 9, p. 305, 2019.

[40] S. Cao, Y. Zhao, S. Feng et al., "Theoretical analysis of InGaAs/InAlAs single-photon avalanche photodiodes," *Nanoscale Research Letters*, vol. 14, no. 1, pp. 2–8, 2019.

[41] L. T. N. Bao and D. N. Thao, "Theoretical investigation of quantum beat of excitons in GaAs/AlGaAs quantum wells," in *The 42nd Vietnam National Conf. on Theoretical Physics (NCTP-42)*, Cantho, Vietnam, 2017.

[42] G. Rezaei, M. R. K. Vahdani, and B. Vaseghi, "Nonlinear optical properties of a hydrogenic impurity in an ellipsoidal finite

potential quantum dot," *Current Applied Physics*, vol. 11, no. 2, pp. 176–181, 2011.

[43] T. Chen, W. Xie, and S. Liang, "The nonlinear optical rectification of an ellipsoidal quantum dot with impurity in the presence of an electric field," *Physica E*, vol. 44, no. 4, pp. 786–790, 2012.

[44] L. Bányai and S. W. Koch, *Semiconductor Quantum Dots*, World Scientific, Singapore, 1st ed. edition, 1993.

[45] R. Jorio, G. D. Saito, M. S. Dresselhaus, and M. S. Dresselhaus, *Raman spectroscopy in graphene related systems*, John Wiley & Sons, 2011.